Calculating terrain indices along streams: A new method for separating stream sides

T. J. Grabs,[1] K. G. Jencso,[2] B. L. McGlynn,[2] and J. Seibert[1,3]

Received 13 March 2010; revised 29 July 2010; accepted 13 August 2010; published 14 December 2010.

[1] There is increasing interest in assessing riparian zones and their hydrological and biogeochemical buffering capacity with indices derived from hydrologic landscape analysis of digital elevation data. Upslope contributing area is a common surrogate for lateral water flows and can be used to assess the variability of local water inflows to riparian zones and streams. However, current geographic information system algorithms do not provide a method for easily separating riparian zone and adjacent upland lateral contributions on each side of the stream. Here we propose a new algorithm to compute side-separated contributions along stream networks. We describe the new algorithm and illustrate the importance of distinguishing between lateral inflows on each side of streams with hillslope–riparian zone–stream hydrologic connectivity results from high-frequency water table data collected in the 22 km^2 Tenderfoot Creek catchment, Montana.

Citation: Grabs, T. J., K. G. Jencso, B. L. McGlynn, and J. Seibert (2010), Calculating terrain indices along streams: A new method for separating stream sides, *Water Resour. Res.*, *46*, W12536, doi:10.1029/2010WR009296.

1. Introduction

[2] Accurate representation of distributed hydrological processes at the watershed scale demands improved predictive tools that can maximize information derived from spatial data sets such as digital elevation models (DEMs). Hydrological terrain analysis based on topography, typically represented by DEMs, can be used to characterize stream networks and riparian zones. Over the past 30 years, various flow algorithms have been developed for estimating the redistribution of water across the landscape based on topography [*O'Callaghan and Mark*, 1984; *Freeman*, 1991; *Quinn et al.*, 1991; *Costa-Cabral and Burges*, 1994; *Tarboton*, 1997; *Gruber and Peckham*, 2009]. These algorithms compute upslope contributing area (a surrogate for shallow groundwater flow) for a specific location in a catchment and also allow quantifying of local lateral contributions entering streams [*McGlynn and Seibert*, 2003]. A shortcoming of these algorithms, however, is that they cannot preserve the information about the side from which local contributions enter a stream. Lateral contributions calculated in this way, thus, represent the total lateral contributions from both sides of a stream. This is problematic because groundwater dynamics and groundwater chemistry can differ considerably between left and right sides of a channel [*Burns et al.*, 1998].

[3] Distinguishing between lateral contributions from opposing sides is also important for assessment of riparian zone function and its influence on catchment scale water chemistry. Riparian zones (RZs) are elongated strips of land directly adjacent to both sides of a stream network. Located at the land-water interface, RZs can be biogeochemical and ecological hotspots [*Gregory et al.*, 1991; *McClain et al.*, 2003] with often distinct soils [*Hill*, 1996] and vegetation [*Jansson et al.*, 2007]. Their location, coupled with their characteristic hydrochemical signature [*Bishop et al.*, 1990; *Hill*, 1990; *Cirmo and McDonnell*, 1997], can give RZs significant potential to "buffer" hillslope groundwater inflows both hydrologically [*McGlynn and McDonnell*, 2003; *Jencso et al.*, 2010] and biogeochemically [*Cirmo and McDonnell*, 1997; *Hooper et al.*, 1998].

[4] *McGlynn and Seibert* [2003] outlined an approach for mapping hydrologic connectivity and riparian buffering based upon terrain indices derived from a DEM in the Maimai catchment, New Zealand. In their approach, potential hydrologic connectivity among hillslopes and riparian zones is characterized by lateral contributing area. Riparian buffering potential along a stream reach is defined as the ratio between riparian and hillslope areas. A limitation of that study is that upslope and riparian areas from both sides were lumped together despite potentially large differences in riparian function and upslope controls on either side along the stream network [*Vidon and Hill*, 2004; *Vidon and Smith*, 2007].

[5] Here we outline a novel method (SIDE; Stream Index Division Equations) that determines the orientation of flow lines (FLs) relative to the streamflow direction to distinguish between stream left and right sides. As an illustrative example we combine this method with a standard flow accumulation algorithm [*Seibert and McGlynn*, 2007] to compute side-separated lateral contributing area per unit stream length (a_c) and riparian buffering ratios (the local ratio of riparian area to total hillslope area, R/H) [*McGlynn and Seibert*, 2003], for the Tenderfoot Creek Experimental Forest, Montana. The utility of the new algorithm is also assessed by comparing a_c values with hillslope–riparian–stream (HRS) water table connectivity

[1]Department of Physical Geography and Quaternary Geology, Stockholm University, Stockholm, Sweden.
[2]Department of Land Resources and Environmental Sciences, Montana State University, Bozeman, Montana, USA.
[3]Also at Department of Geography, University of Zürich, Zurich, Switzerland.

Copyright 2010 by the American Geophysical Union.
0043-1397/10/2010WR009296

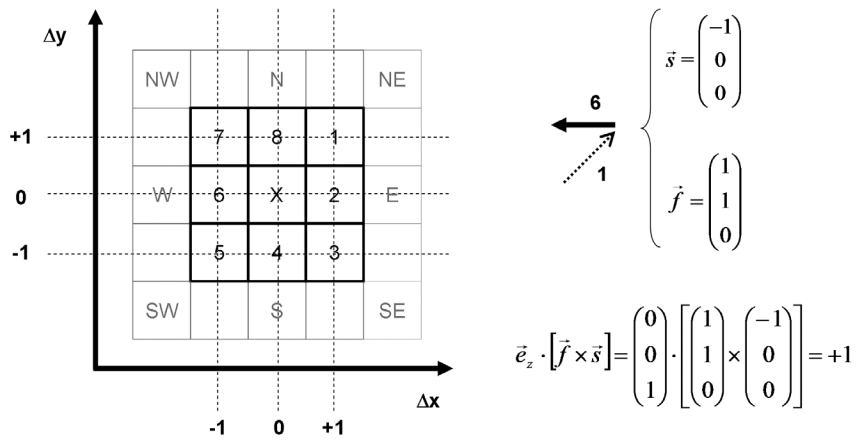

Figure 1. Stream flow direction grid. Directions relative to center grid cell X are coded from 1 to 8 clockwise from northeast (NE) to north (N). The corresponding vector notation is illustrated for flow line vector $\vec{f}$ in direction 1 (dotted arrow) and for streamflow vector $\vec{s}$ in direction 6 (plain arrow). Calculating the cross product $\vec{f} \times \vec{s}$ reveals a positive z component and therefore flow line vector $\vec{f}$ is located on the left side relative to stream vector $\vec{s}$.

dynamics on either side of the stream network at 24 transects of groundwater recording wells [*Jencso et al.*, 2009].

2. New Algorithm

2.1. Stream Side Determination

[6] All flow routing algorithms estimate (often implicitly) flow fields for computing the downslope accumulation of area or other landscape attributes. Our new SIDE method determines the orientation of flow fields relative to a stream network. This is achieved by a stepwise comparison of flow lines (FLs; vectors of the flow field directed to streams) with streamflow directions. Performing these steps requires a DEM and a streamflow direction map (SDM) which consists of a network of connected stream vectors. Regularly gridded data is used in this study although the same methodology is applicable to other data structures. Stream directions in a gridded SDM are represented by grid cells with integer values that correspond to different flow directions (Figure 1).

[7] The SIDE algorithm attributes FLs to each side of a stream channel based on geometric calculations. Once the orientations of all FLs are determined, other upslope landscape attributes that are linked to the stream network via FLs can be accordingly assigned to left or right stream sides.

[8] The first step for calculating FL orientation is to determine the corresponding FL and streamflow directions, $\vec{f}_k$ and $\vec{s}_{k,0}$, respectively, for every grid cell of the DEM that drains into one or several downslope SDM grid cells. Additionally, all streamflow vectors $\vec{s}_{k,i}$ of the upstream SDM grid cells that are directly connected to $\vec{s}_{k,0}$ are located. The second step is to determine the orientation of the FLs relative to the streamflow direction (Figure 2). For this the cross products $\vec{c}_{k,i}$ of all pairs of each FL direction $\vec{f}_k$ with different streamflow directions $\vec{s}_{k,i}$ are calculated as

$$\vec{c}_{k,i} = \vec{f}_k \times \vec{s}_{k,i}. \quad (1)$$

[9] Since $\vec{f}_k$ and $\vec{s}_{k,i}$ are horizontal vectors with z components equal to zero, the resulting cross products $\vec{c}_i$ are

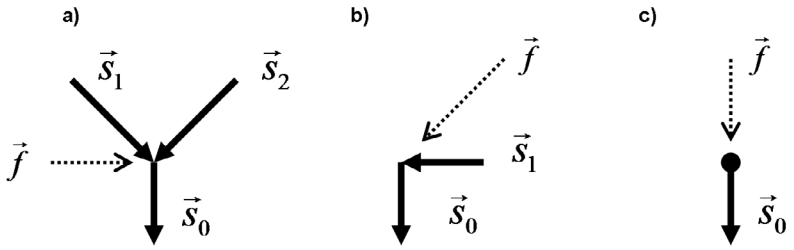

Figure 2. Different configurations of flow lines $\vec{f}$ (dotted arrows) and stream vectors $\vec{s}_i$, i ≥ 0 (plain arrows). (a) Stream junction: In this example, the flow line $\vec{f}$ is located on the right stream side because it is on the right side relative to all stream vectors $\vec{s}_i$. (b) Sharp stream bend: In this example $\vec{f}$ is on the left side relative to $\vec{s}_0$ and on the right side relative to $\vec{s}_1$ and therefore on the outer side of the bend. Since the cross product $\vec{s}_1 \times \vec{s}_2$ has a positive z component the inner bend must be located on the left stream side and $\vec{f}$, hence, is on the right stream side. (c) Channel head: In this example the orientation of the flow line $\vec{f}$ relative to $\vec{s}_0$ is not definable.

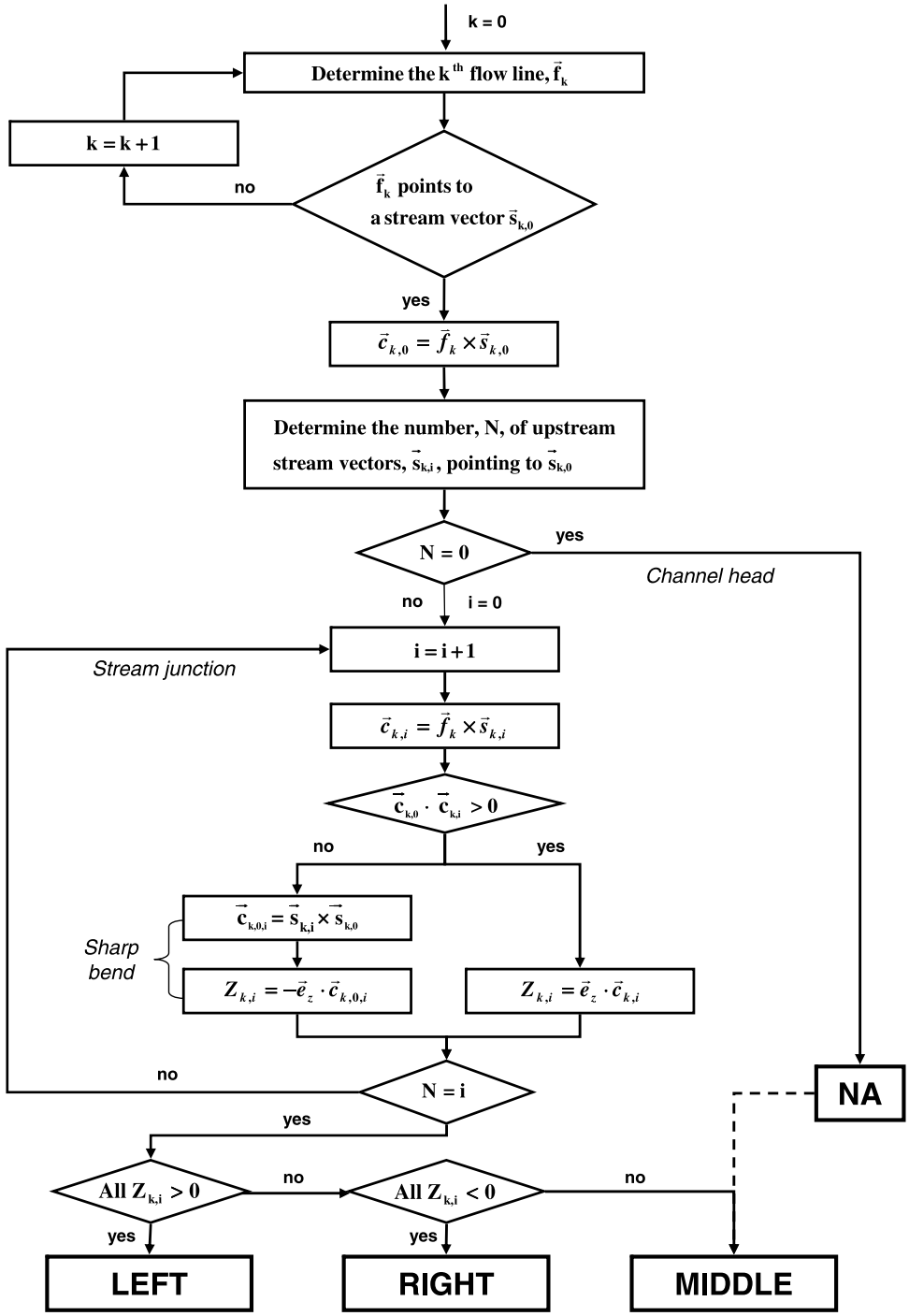

Figure 3. Flowchart illustrating the determination of a hillslope position. Symbols are defined in the notations list.

perpendicular to the map plane and only their z components $Z_{k,i}$ are different from zero, except when $\vec{f}_k$ and $\vec{s}_{k,i}$ are parallel. The z components are calculated as

$$Z_{k,i} = \vec{e}_z \cdot \vec{c}_{k,i}. \quad (2)$$

[10] The sign of $Z_{k,i}$ indicates the orientation of the corresponding FL relative to the streamflow direction. If left and right are defined in direction of stream vector $\vec{s}_0$ (i.e., looking in the downstream direction of the stream), then a negative $Z_{k,i}$ indicates that the corresponding FL is oriented right relative to the streamflow. Similarly, a positive $Z_{k,i}$ value indicates that the corresponding FL is oriented left. If all $Z_{k,i}$ values of all cross products have the same sign then the orientation of the FL can be directly inferred from the common sign of the $Z_{k,i}$ values.

[11] Occasionally FL orientations (and the corresponding stream sides) cannot be resolved directly and additional steps must be taken. These special cases occur at locations where the z components of the cross products have opposite

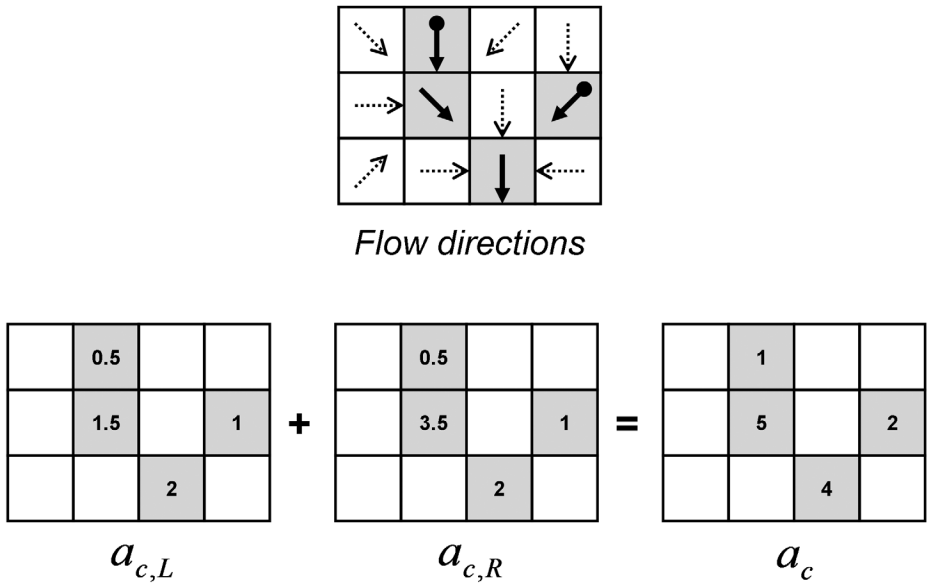

Figure 4. Illustrations of a flow direction map and three maps showing values of specific lateral contributing area, a_c. The flow direction map shows hillslope and stream flow directions. The three lower maps feature a_c entering the stream from left ($a_{c,L}$) and a_c entering the stream from right ($a_{c,R}$) as well as the total a_c, which is the sum of $a_{c,L}$ and $a_{c,R}$. For simplicity, the a_c values presented in this illustration are equal to the number of contributing grid cells.

signs, are equal to zero, or where the FLs point to channel heads.

[12] The first exception occurs when two stream directions, $\vec{s}_{k,0}$ and $\vec{s}_{k,i}$, form a sharp bend with an inner angle equal to or less than 90° (Figure 2). In this case the z components of $\vec{c}_{k,0}$ and $\vec{c}_{k,i}$ have opposite signs or one z component is equal to zero. If the FL was located on the inner side of the sharp bend then both z components would necessarily have the same sign and the orientation of the FL relative to the stream could be calculated as described previously. However, in this case the FL is located on the outer side of the bend and the z components of $\vec{c}_{k,0}$ and $\vec{c}_{k,i}$ have different signs. The solution to this problem is to find the position of $\vec{s}_{k,i}$ relative to $\vec{s}_{k,0}$ by calculating the cross product $\vec{c}_{k,0,i}$ of the two stream vectors as

$$\vec{c}_{k,0,i} = \vec{s}_{k,i} \times \vec{s}_{k,0}. \tag{3}$$

[13] If the z component of $\vec{c}_{k,0,i}$ is negative then $\vec{s}_{k,i}$ lies on the right side relative to $\vec{s}_{k,0}$. The inner side of the sharp bend is therefore oriented right relative to $\vec{s}_{k,0}$. However, the FL is located on the outer side of the sharp bend. Hence, the FL has to be oriented left to the stream while the opposite is true in case of a positive z component of $\vec{c}_{k,0,i}$. More generally, the side of the RZ is indicated by the sign of $Z_{k,i}$, which is calculated by multiplying the z components of $\vec{c}_{k,0,i}$ by minus one as in

$$Z_{k,i} = -\vec{e}_z \cdot \vec{c}_{k,0,i}. \tag{4}$$

[14] Stream junctions represent another special case because the assessment of FL orientations requires comparing two or more upstream streamflow directions with the streamflow direction directly downstream of the junction. For computation, the junctions are first subdivided into a number of stream bends and treated individually. The subdivided stream bends correspond to all possible combinations of the downstream stream vector $\vec{s}_{k,0}$ with one of the upstream stream vectors $\vec{s}_{k,i}$. The side of each FL pointing towards the junction can then be determined relative to each bend, that is, relative to every combination of $\vec{s}_{k,0}$ and $\vec{s}_{k,i}$, in the same way as described previously. In the end, the FL orientation (as well as the side of the corresponding RZ) relative to the stream junction corresponds to its orientation relative to all individual stream bends. If the FL is oriented left relative to certain streamflow directions and, simultaneously, right relative to others, then the FL is actually located in the middle of two confluences joining at a stream junction.

[15] Channel heads are a third special case because they represent singularities where the orientation of FLs is undetermined ("NA" in Figure 3). As a practical solution to avoid missing values, FLs pointing to channel heads are treated as if they were pointing exactly to the middle of two confluences and are attributed to both stream sides.

2.2. Calculation of Lateral Contributing Areas

[16] After the relative orientation of all FLs is determined for all cases (Figure 3), the values of upslope contributing areas A_c (m^2) calculated from the flow accumulation algorithm are assigned to the respective sides. Note that A_c as we use it in this paper only refers to the local contribution of area to a stream segment and does not include any area entering from upstream stream segments. Length-specific values of contributing area a_c (m^2/m) were calculated by dividing A_c values by the local stream segment lengths Δl (m); grid size in cardinal or diagonal direction. The result is two maps representing the specific contributing areas entering the stream from left, $a_{c,L}$, and right, $a_{c,R}$ (Figure 4). In most cases the assignment of the entering area to one of the sides is straight-forward (see flowchart cases LEFT and RIGHT, Figure 3). In special cases where a FL points to a

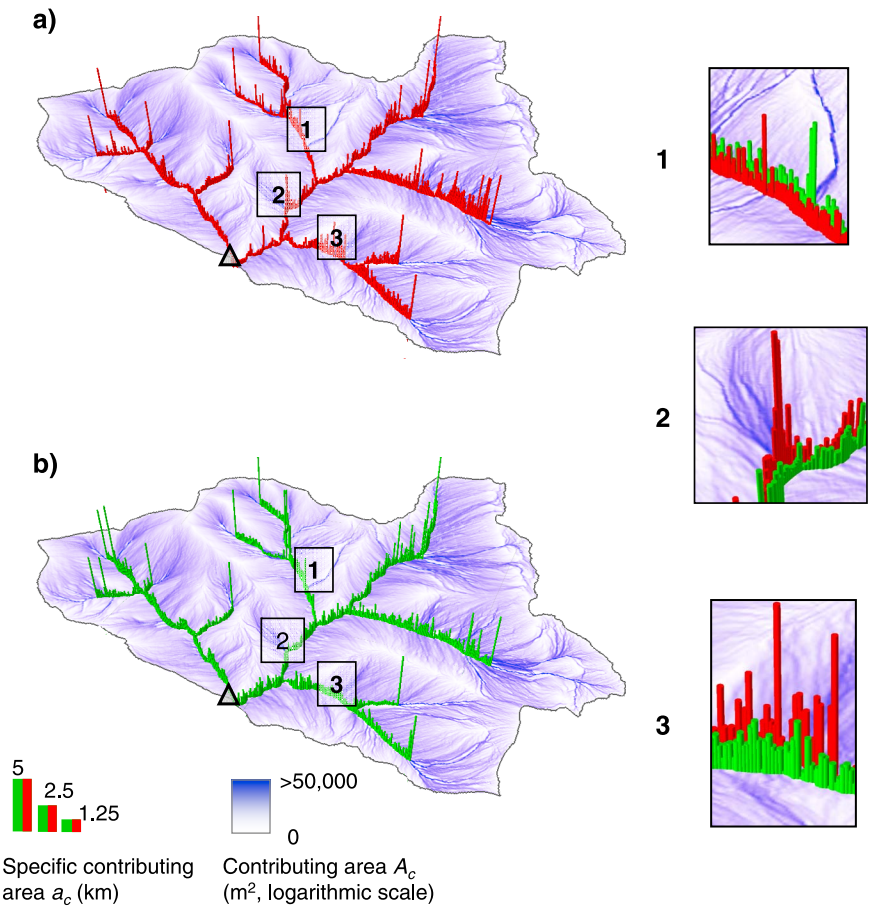

Figure 5. Spatial representation of contributing area *Ac* (blue-shaded flow lines) and side-separated specific contributing area values a_c from left (green bars) and right (red bars) stream sides. (a) Illustrates the specific contribution area values from right stream sides, $a_{c,R}$, while (b) shows the contributions from left stream sides, $a_{c,L}$. Insets (1, 2, and 3) represent close-up views of selected stream locations in the catchment. Triangles mark the outlet of the Tenderfoot Creek experimental catchment.

channel head or is located between two confluents to a junction (Figure 3, MIDDLE case) the area is apportioned equally between the two sides. While it may be argued that the first grid cells of a stream (i.e., the channel heads) do not have a left or right side, counting half of the area to $a_{c,L}$, respectively $a_{c,R}$, is a pragmatic solution to avoid missing values. The total local contributing area entering the stream at a certain location, a_c (m^2/m) can easily be calculated as the sum of the contributions from the two sides as

$$a_c = a_{c,L} + a_{c,R}. \quad (5)$$

[17] The new algorithm has been implemented in the open source geographic information system (GIS) software SAGA [*Conrad*, 2007; *Böhner et al.*, 2008]. Computationally the algorithm is similarly demanding as when applying a flow routing algorithm only to grid cells that are directly adjacent to the stream network. Since the number of such riparian grid cells is usually small compared to the total amount of grid cells in a DEM, the additional computational load is small as well. For instance, applying the SIDE method in combination with the MD∞ algorithm [*Seibert and McGlynn*, 2007] to a 570 × 832 sized DEM (with 2.3×10^6 nonmissing values) and the corresponding SDM (with 1.5×10^3 nonmissing values) took less than 2 seconds on a notebook computer with 2 Gb of virtual memory and a 2.2 Ghz Intel Pentium™ 2 Xeon processor.

3. Case Study

[18] To demonstrate the new SIDE algorithm and the value of separating the stream into left and right sides, data from the Tenderfoot Creek Experimental Forest (TCEF) was used. TCEF is located in the Little Belt Mountains of the Lewis and Clark National Forest in Central Montana. The research area consists of seven gauged catchments that form the headwaters of Tenderfoot Creek (22.8 km^2), which drains into Smith River, a tributary of the Missouri River. Catchment headwater zones are typified by moderately sloping (ave. slope ~8°), extensive (up to 1200 m long) hillslopes and variable width riparian zones. Approaching the main stem of Tenderfoot Creek the streams become more incised, hillslopes become shorter (<500 m) and steeper (ave. slope ~20°), and riparian areas narrow compared to the catchment headwaters. Stream sides and side-separated indices were calculated from a 10 m DEM (Figure 5) using the new SIDE algorithm and the MD∞ flow accumulation method [*Seibert and McGlynn*, 2007] to compute upslope area. The stream network and the stream direction map were derived from the DEM by applying various parameters (Table 1) in the

Table 1. Parameters Used in the SAGA "Channel Network" Module

Parameter	Value
Minimum Segment Length, grid cells	10
Tracing: Maximum Divergence, grid cells	5
Initiation Threshold, m^2	40,000

"Channel Network" module in SAGA [*Conrad*, 2007; *Böhner et al.*, 2008], using the DEM and a map of upslope area. A threshold area of 40 ha defined stream initiation. The derived channel heads and the stream network were further corroborated with results from field reconnaissance [*Jencso et al.*, 2009].

[19] To analyze the effect of the side-separated calculations, the specific lateral contributing areas, which were computed using the new algorithm, were compared by visual assessment of $a_{c,R}$ and $a_{c,L}$ maps and by plotting $a_{c,R}$ against $a_{c,L}$. Furthermore, riparian buffer ratios [*McGlynn and Seibert*, 2003] with their associated catchment-wide, area-weighted distribution functions were computed to exemplify the use of the SIDE method to derive composite terrain indices. The R/H index was chosen over other composite terrain indices, such as the topographic wetness index [*Beven and Kirkby*, 1979], because both components (R and H) are calculated based on flow fields and do not involve local components (e.g., local slope). The riparian buffer ratio R/H was here defined as the ratio between area of the lateral contributing riparian area, R, and the entire lateral contribution, H. The TCEF lateral riparian areas were mapped based on the field relationship described by *Jencso et al.* [2009]. Landscape analysis–derived riparian area was delineated as all area less than 2 m in elevation above the stream network. To compare the landscape analysis–derived riparian widths to actual riparian widths at TCEF, *Jencso et al.* [2009] surveyed 90 riparian cross sections in Stringer Creek, Spring Park Creek, and Tenderfoot Creek. A regression relationship (r^2 = 0.97) corroborated their terrain-based riparian extent mapping [*Jencso et al.*, 2009]. The total and side-separated lateral contributions, H, used in the R/H ratio correspond to the previously computed $a_{c,L}$, $a_{c,R}$, and a_c ($a_c = a_{c,L} + a_{c,R}$) values. Total and side-separated riparian lateral contributions, R, were calculated by applying the SIDE method and the MD∞ flow accumulation algorithm of *Seibert and McGlynn* [2007] on the DEM, excluding the parts outside the mapped riparian area.

[20] Finally we report on results of hillslope connectivity measured using shallow groundwater recording in 24 transects and show how side-separated a_c values improved the correlations between this terrain index and water table connectivity across the 24 transects. Hydrologic connectivity between HRS zones was inferred from the presence of saturation measured in well transects spanning the hillslope, toeslope, and riparian positions. A HRS hydrologic connection was defined as a time interval during which stream flow occurred and both the riparian and adjacent hillslope wells recorded water levels above bedrock. More detailed information about the experimental design and hydrological connectivity was presented by *Jencso et al.* [2009].

4. Results

[21] Side-separated lateral contributions to the stream network were calculated for TCEF using the SIDE method (Figure 5). The contributions from the two sides generally varied considerably. Plotting $a_{c,L}$ against $a_{c,R}$ clearly demonstrated that contributions from two sides at different locations along the stream network differed considerably (Figure 6), apart from the channel heads (area labeled "1" in Figure 6). This also implies that total local contributing area a_c cannot be a proxy for side-separated local contributing areas. There are two patterns in the correlation

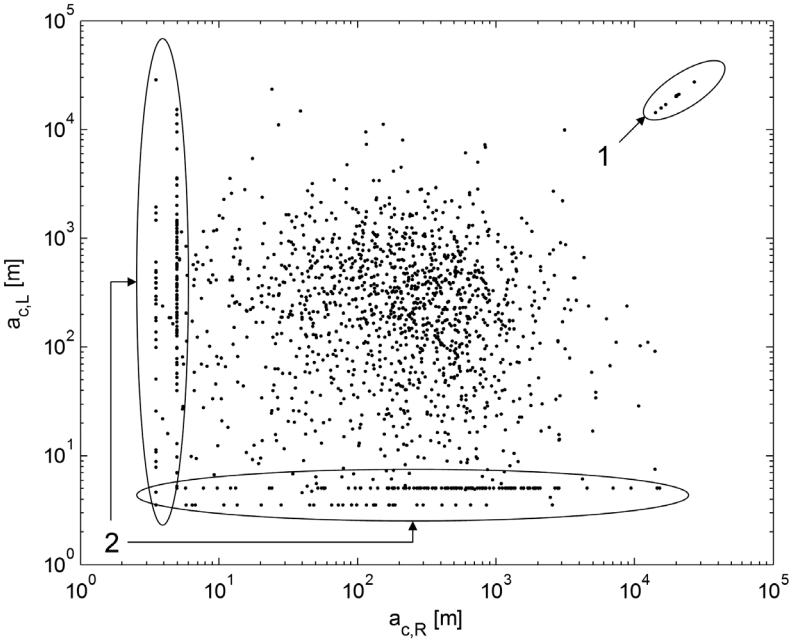

Figure 6. Scatter plot of right specific lateral contributing areas ($a_{c,R}$) versus their counterparts on the left stream side ($a_{c,L}$) along the stream network of the 23 km^2 Tenderfoot Creek Experimental Forest catchment. Areas labeled 1 and 2 are explained in the text.

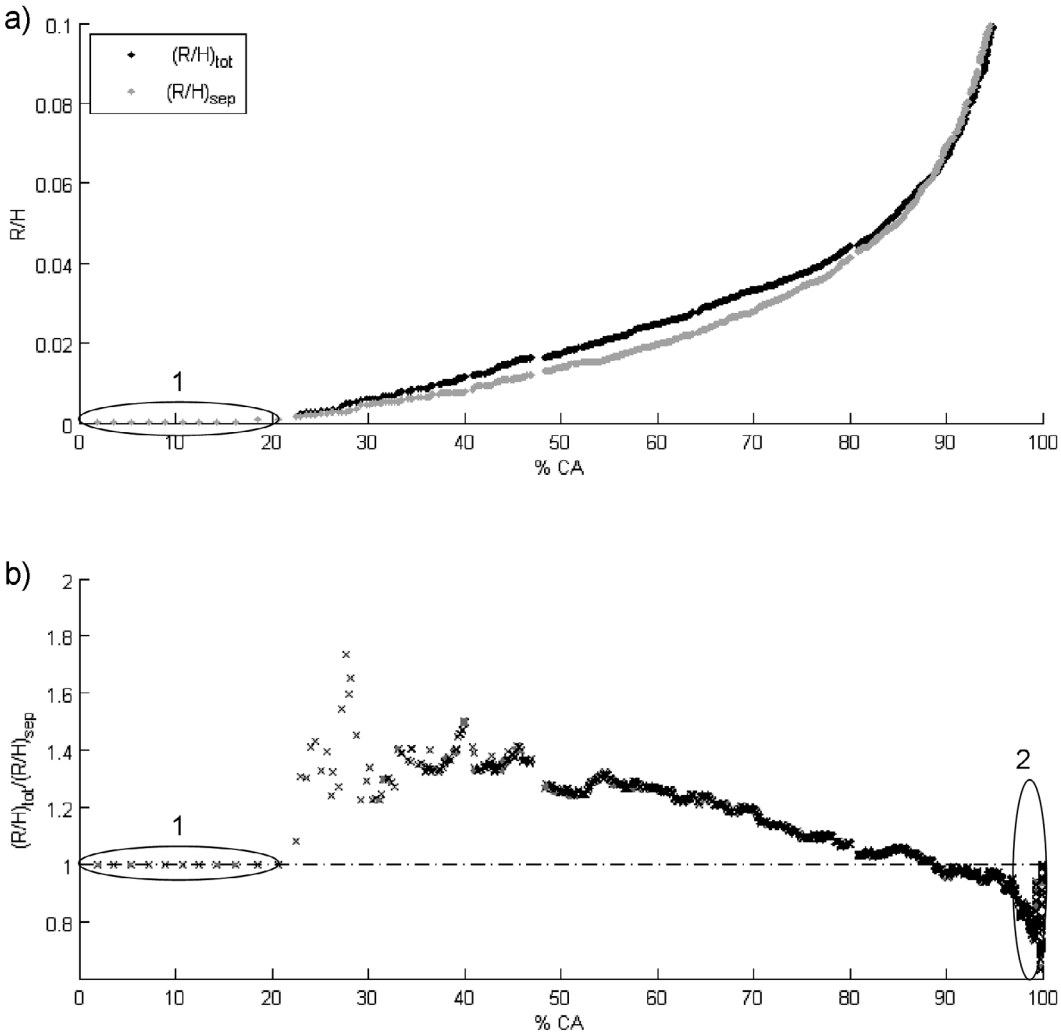

Figure 7. Comparison of riparian-hillslope ratios (R/H) calculated based on total and side-separated values. (a) Cumulative area-weighted distributions of riparian-hillslope ratios $(R/H)_{sep}$ and $(R/H)_{tot}$. (b) Ratios of the above distribution functions. Areas labeled 1 and 2 are explained in the text.

plot which might need further explanation. The apparently well-correlated points in the upper right part of the figure (area labeled "1" in Figure 6) correspond to channel heads. For those cells there is a perfect, but trivial, correlation because the total contributing area for these grid cells was partitioned equally according to the special case where FLs point to channel heads. The linear patterns (areas labeled "2" in Figure 6) are caused by stream cells receiving the minimal contributing area (a half cell) normalized by the stream length in either cardinal or diagonal directions. Such stream cells are typically found in locations where divergent slopes are adjacent to the stream. Here the lateral contribution can consist of just the stream cell itself, which means that only half of the $100m^2$ grid cell is contributing from one side (streams are assumed to be in the center of the delineated stream cells).

[22] In addition to lateral contributing areas, composite flow-related terrain indices that are calculated along streams are also potentially sensitive to the separation of lateral contributions. This was tested using the R/H index computed for TCEF. We calculated area-weighted distribution functions of the R/H index to compare our new method to the standard method. The results differed considerably for those values calculated from side-separated a_c values and those calculated from total a_c values (Figure 7a). Generally, the R/H indices calculated from total a_c values were larger than those obtained from side-separated $a_{c,R}$ and $a_{c,L}$ values. For instance, the R/H distribution derived from the side-separation algorithm indicates that 50% of the catchment area enters the stream network along segments where the R/H index is less than 0.014. In contrast the R/H distribution derived from total a_c values overestimates this quantity by a factor of approximately 1.3, which is indicated by the ratios of the two distributions (Figure 7b). Overall, using total a_c values, the area-weighted R/H distribution can be up to 1.8 times or 80% higher than predicted when using side-separated a_c values (Figure 7b).

[23] We further assessed the utility of the SIDE method for predicting local hydrologic observations from the Stringer Creek catchment, a subcatchment of TCEF. When comparing a_c values to the time percentage for HRS water table connectivity, the degree of correlation largely depended on whether total or side-separated a_c values were used (Figure 8). A poor relationship ($r^2 = 0.42$) was observed when comparing total

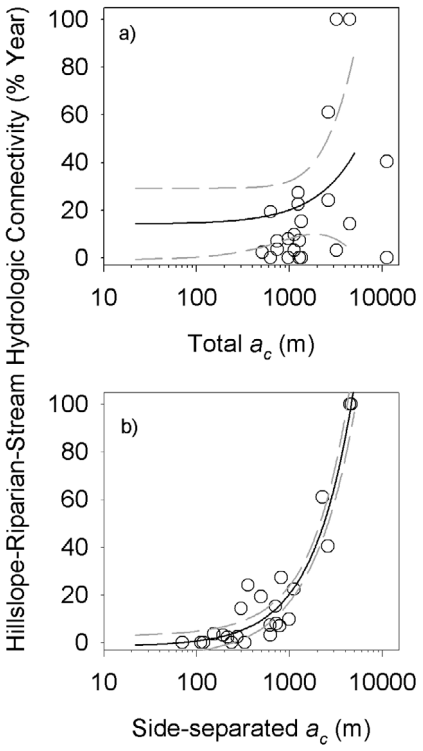

Figure 8. Hillslope a_c regressed against the percentage of the water-year that a hillslope-riparian-stream water table connection existed for 24 well transects. (a) Total a_c from both sides of a transect cross-section and (b) a_c separated into left and right sides of the stream. A connection occurred when there was stream flow and when water levels were recorded in both the riparian and hillslope wells (modified from *Jencso et al.* [2009]).

a_c for each transect cross-section against HRS water table connectivity (Figure 8a). When replacing total a_c with side-separated a_c values the correlation between specific lateral contributing area and HRS water table connectivity improved considerably ($r^2 = 0.91$, Figure 8b).

[24] As an example, more detailed results are presented for Stringer Creek transect 5. The total A_c for the stream cell at this transect is about 48,000 m^2 which corresponds to a total specific a_c of 4800 m. However, the two stream sides contribute a disproportionate amount of area to the total value. The western (right) side is located at the base of a convergent hillslope (Figure 9). It has the largest side-separated a_c ($a_{c,R} \cong 4600$ m) of all 24 TCEF transects under observation, a wide riparian zone (16.5 m) and ~20.5° hillslopes. The eastern side of transect 5 (left side of map in Figure 9) is located along a moderate gradient (~26°), divergent hillslope ($a_{c,L} \cong 200$ m) with a 7.7 m wide riparian zone. On the western side of transect 5 (right side of map in Figure 9) HRS water table connectivity was observed for the entire water year while on the eastern side water table connectivity was transient during the same period and only occurred on 11 days with the largest snowmelt and rain events.

5. Discussion

[25] In general, left and right lateral hillslope contributions at various stream locations differed substantially (Figure 6). This is plausible as values of $a_{c,R}$ would only be strongly related to values of $a_{c,L}$ in catchments with either highly symmetric or highly asymmetric local lateral inflows along the entire stream network. Such catchment structures are the exception and would be very unusual. Using total a_c instead of side-separated values can therefore give misleading results. We suggest that traditional GIS algorithms that are only capable of deriving total a_c are not appropriate for estimating variations in lateral contributions to the stream or for characterizing riparian zones.

[26] The distribution of R/H indices varied systematically depending on whether total or side-separated a_c values were used. Using total a_c values caused substantial overestimation and could lead to misconceptions when attempting to characterize riparian zone and their distributions and buffering potential. The previously described distinct patterns associated with channel heads and minimal contributing areas (number labeled areas in Figure 6) are related to the

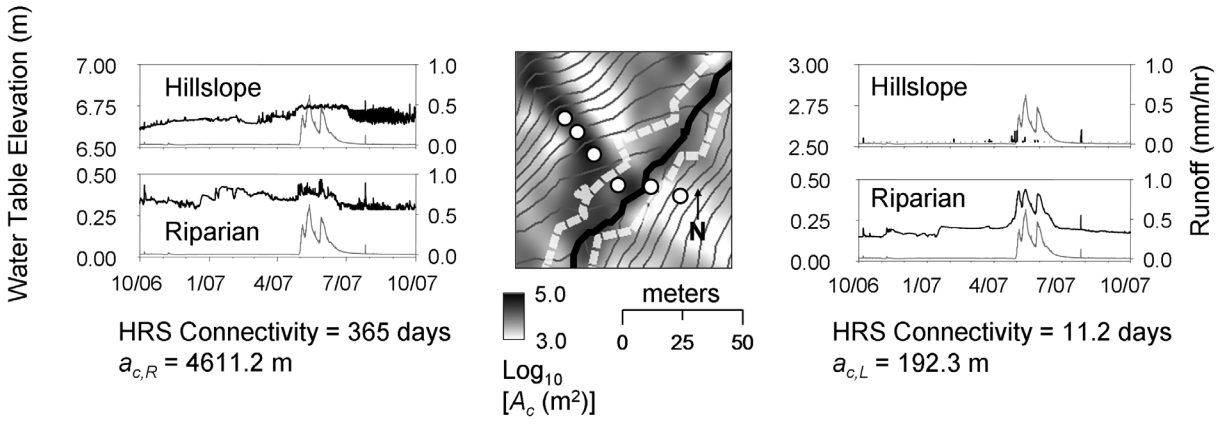

Figure 9. Stringer Creek transect 5 east and west hillslope and riparian water table (black lines, elevation is relative to local datum) and runoff (gray lines) dynamics. Specific area for each side of the transect and the total time of hillslope-riparian-stream connectivity (days) during the 2007 water year are listed below each time series. The map in the middle depicts the transects contributing area A_c (dark shading corresponds to high values of A_c and light shading indicates low values of A_c), contour lines (gray lines), riparian zone extents (white dashed lines), well locations (white circles), and stream position (black line).

resolution in the DEM cell size and the flow accumulation algorithm used. The same artifacts also emerge as distinct clusters in plots of area-weighted R/H distributions. Channel heads emerge as clusters when plotting the distributions (labeled as "1" in Figure 7a) and when plotting the ratios of the distributions (Figure 7b, label "1"). TCEF channel heads are located in steep terrain with narrow riparian zones of only a few square meters. Since stream channels are initiated at high values of A_c where riparian zones are narrow, the corresponding R/H ratios are close to 0. Moreover, R/H values calculated using the side-separating algorithm are equal to those of the standard algorithm because the side-separating algorithm divides riparian and hillslope a_c values equally between left and right at channel heads.

[27] Apart from artifacts, ratios of the two distributions $(R/H)_{sep}/(R/H)_{tot}$ also reveal that the distributions are skewed towards the higher values of R/H. At this end of the R/H spectrum the side-separating algorithm predicts higher R/H values than the standard algorithm. Many of the high R/H ratios are in fact related to riparian zones connected to little or no upslope parts of the catchment and emerge as clusters (area labeled with "2" in Figure 7). Using the standard algorithm, low hillslope a_c values from one side often are compensated by higher hillslope a_c values from the other side and, thus, high R/H ratios occur much less often. The lumping of hillslope and riparian a_c values affects the entire distribution of R/H values and leads to inaccurate characterization. The comparatively higher R/H values predicted by the side-separating algorithm are hence more realistic. We further suppose, without having tested it in detail yet, that applying the SIDE method to derive other composite flow-related terrain indices along streams (e.g., the topographic wetness index [*Kirkby*, 1975]) would lead to similarly profound consequences compared to using a standard algorithm.

[28] Lateral contributions of hillslope and riparian areas on the opposite sides of the stream also varied considerably for all 24 transects with detailed groundwater observations. A closer look at individual transects, such as transect 5 (Figure 9), indicates that differential convergence and divergence of catchment topography and hillslope lengths are among the most likely causes for the observed differences. These differences were also directly reflected by HRS water table dynamics. For all 24 transects, total a_c calculated with standard methods was not a suitable proxy for both streams sites and only weakly related to HRS water table connectivity whereas the opposite was found when using side-separated a_c values. The practical application of our SIDE algorithm hence enabled *Jencso et al.* [2009] to estimate the amount of the stream network connected to its uplands through time and to upscale these predictions to the entire catchment.

[29] The proposed SIDE method is compatible with any existing flow accumulation algorithm and can, in its current implementation, be combined with the D8 [*O'Callaghan and Mark*, 1984], MD8 [*Quinn et al.*, 1991], D∞ [*Tarboton*, 1997], and MD∞ [*Seibert and McGlynn*, 2007] algorithms. Flow accumulation algorithms not only allow computation of the size of upslope contributing areas, but can also be used to compute average values of upslope landscape attributes. For instance, the SIDE method would allow calculation of the average forest coverage of upslope land portions for each stream cell on both stream sides. More generally, all calculations that fall into the broad category of flow algebra [*Tarboton and Baker*, 2008] can be combined with the proposed SIDE method to provide more meaningful indices for stream segments and riparian zones.

[30] The SIDE algorithm can be applied to streams in any type of environment and is only limited by the accuracy of the stream network position and by the chosen flow accumulation algorithm. In particular, topographically-derived flow fields can differ from actual flow fields as a result of heterogeneous soils, bedrock topography, or temporally-varying flow directions [*Hinton et al.*, 1993; *Devito et al.*, 1996; *Freer et al.*, 2002]. There is, however, a potential to overcome at least some these limitations by the use of distributed hydrological models to derive flow fields. Such an approach has been demonstrated by *Grabs et al.* [2009], who used a distributed hydrological model to simulate flow fields in flat areas based on hydraulic gradients rather than on terrain slope.

6. Concluding Remarks

[31] We outline a new algorithm that is widely applicable and useful for interpreting, routing, and assessing a wide variety of terrain analysis indices related to stream networks and hydrology. These include, but are not limited to, hillslope accumulated area contributing to streams, riparian buffering, wetness indices, lateral stream inflows of water and associated constituents, and any indices where orientation relative to the stream network is important. The new algorithm has been implemented as a module for the open source GIS software SAGA [*Conrad*, 2007; *Böhner et al.*, 2008] and can easily be used by others. The source code of the SIDE algorithm is included as supplementary material, while a compiled SAGA-module along with usage instructions can be found at the main author's website (http://thomasgrabs.com/side-algorithm).

[32] The new SIDE algorithm addresses an important shortcoming of standard hydrological landscape analysis where the possibility of calculating side-separated lateral contributions to streams so far has been lacking. The side-separated calculations are crucial for a meaningful characterization of the riparian zone through terrain indices and provide a basis for an efficient up-scaling of riparian-controlled processes to the landscape scale.

Notation

A_c	Lateral contributing area, m^2
a_c	Specific lateral contributing area, m
$a_{c,L}$	Left specific lateral contributing area, m
$a_{c,R}$	Right specific lateral contributing area, m
$\vec{c}$	Cross product, m^2
Δl	Grid size in cardinal or diagonal direction, m
$\vec{e}_z$	Unit vector in z direction (vertical), -
i	Index of (upstream) tributaries to a stream segment, -
k	Index of riparian (flow line) vectors, -
NA	Missing value, -
$\vec{f}$	Flow line direction (vector), m
H	Hillslope area, m^2
R	Riparian area, m^2
R/H	Riparian-hillslope ratio, -
$\vec{s}$	Streamflow direction (vector), m
Z	Z component of cross-products, m^2

[33] **Acknowledgments.** This project was partly funded by the Swedish Research Council (VR, grant 2005-4289).

References

Beven, K., and M. Kirkby (1979), A physically based, variable contributing area model of basin hydrology, *Hydrol. Sci. Bull.*, *24*, 43–69.

Bishop, K. H., H. Grip, and A. O'Neill (1990), The origins of acid runoff in a hillslope during storm events, *J. Hydrol.*, *116*, 35–61.

Böhner, J., T. Blaschke, and L. Montanarella (Eds.) (2008), *SAGA: System for an Automated Geographical Analysis*, Inst. Geogr., Univ. Hamburg, Hamburg, Ger.

Burns, D. A., R. P. Hooper, J. J. McDonnell, J. E. Freer, C. Kendall, and K. Beven (1998), Base cation concentrations in subsurface flow from a forested hillslope: The role of flushing frequency, *Water Resour. Res.*, *34*, 3535–3544, doi:10.1029/98WR02450.

Cirmo, C. P., and J. J. McDonnell (1997), Linking the hydrologic and biogeochemical controls of nitrogen transport in near-stream zones of temperate-forested catchments: A review, *J. Hydrol.*, *199*, 88–120.

Conrad, O. (2007), SAGA - Entwurf, Funktionsumfang und Anwendung eines Systems für Automatisierte Geowissenschaftliche Analysen, Electronic doctoral dissertation, 221 pp., Univ. Göttingen, Göttingen, Ger.

Costa-Cabral, M. C., and S. J. Burges (1994), Digital elevation model networks (DEMON): A model of flow over hillslopes for computation of contributing and dispersal areas, *Water Resour. Res.*, *30*, 1681–1692, doi:10.1029/93WR03512.

Devito, K. J., A. R. Hill, and N. Roulet (1996), Groundwater-surface water interactions in headwater forested wetlands of the Canadian Shield, *J. Hydrol.*, *181*, 127–147.

Freeman, T. G. (1991), Calculating catchment area with divergent flow based on a regular grid, *Comput. Geosci.*, *17*, 413–422.

Freer, J., J. J. McDonnell, K. J. Beven, N. E. Peters, D. A. Burns, R. P. Hooper, B. Aulenbach, and C. Kendall (2002), The role of bedrock topography on subsurface storm flow, *Water Resour. Res.*, *38*(12), 1269, doi:10.1029/2001WR000872.

Grabs, T., J. Seibert, K. Bishop, and H. Laudon (2009), Modeling spatial patterns of saturated areas: A comparison of the topographic wetness index and a dynamic distributed model, *J. Hydrol.*, *373*, 15–23, doi:10.1016/j.jhydrol.2009.03.031.

Gregory, S. V., F. J. Swanson, W. A. McKee, and K. W. Cummins (1991), An ecosystem perspective of riparian zones, *BioScience*, *41*, 540–551.

Gruber, S., and S. Peckham (2009), Land-Surface Parameters and Objects in Hydrology, in *Geomorphometry: Concepts, Software, Applications*, edited by T. Hengl and H. I. Reuter, pp. 293–308, Elsevier Science, Amsterdam.

Hill, A. (1990), Ground water flow paths in relation to nitrogen chemistry in the near-stream zone, *Hydrobiologia*, *206*, 39–52.

Hill, A. R. (1996), Nitrate removal in stream riparian zones, *J. Environ. Qual.*, *25*, 743–755.

Hinton, M. J., S. L. Schiff, and M. C. English (1993), Physical properties governing groundwater flow in a glacial till catchment, *J. Hydrol.*, *142*, 229–249.

Hooper, R. P., B. T. Aulenbach, D. A. Burns, J. McDonnell, J. Freer, C. Kendall, and K. Beven (1998), Riparian control of stream-water chemistry: Implications for hydrochemical basin models, *IAHS Publ.*, *248*, 451–458.

Jansson, R., H. Laudon, E. Johansson, and C. Augspurger (2007), The importance of groundwater discharge for plant species number in riparian zones, *Ecology*, *88*, 131–139.

Jencso, K. G., B. L. McGlynn, M. N. Gooseff, S. M. Wondzell, K. E. Bencala, and L. A. Marshall (2009), Hydrologic connectivity between landscapes and streams: Transferring reach-and plot-scale understanding to the catchment scale, *Water Resour. Res.*, *45*, W04428, doi:10.1029/2008WR007225.

Jencso, K. G., B. L. McGlynn, M. N. Gooseff, K. E. Bencala, and S. M. Wondzell (2010), Hillslope hydrologic connectivity controls riparian groundwater turnover: Implications of catchment structure for riparian buffering and stream water sources, *Water Resour. Res.*, doi:10.1029/2009WR008818, in press.

Kirkby, M. J. (1975), Hydrograph modeling strategies, in *Processes in Physical and Human Geography: Bristol Essays*, edited by R. Peel et al., pp. 69–90, Heinemann, London, U.K.

McClain, M. E., et al. (2003), Biogeochemical hot spots and hot moments at the interface of terrestrial and aquatic ecosystems, *Ecosystems*, *6*, 301–312.

McGlynn, B. L., and J. J. McDonnell (2003), Quantifying the relative contributions of riparian and hillslope zones to catchment runoff, *Water Resour. Res.*, *39*(11), 1310, doi:10.1029/2003WR002091.

McGlynn, B. L., and J. Seibert (2003), Distributed assessment of contributing area and riparian buffering along stream networks, *Water Resour. Res.*, *39*(4), 1082, doi:10.1029/2002WR001521.

O'Callaghan, J. F., and D. M. Mark (1984), The extraction of drainage networks from digital elevation data, *Comput. Vision Graphics Image Process.*, *28*, 323–344.

Quinn, P., K. Beven, P. Chevallier, and O. Planchon (1991), The prediction of hillslope flow paths for distributed hydrological modeling using digital terrain models, *Hydrol. Processes*, *5*, 59–79.

Seibert, J., and B. L. McGlynn (2007), A new triangular multiple flow direction algorithm for computing upslope areas from gridded digital elevation models, *Water Resour. Res.*, *43*, W04501, doi:10.1029/2006WR005128.

Tarboton, D. G. (1997), A new method for the determination of flow directions and upslope areas in grid digital elevation models, *Water Resour. Res.*, *33*, 309–319, doi:10.1029/96WR03137.

Tarboton, D. G., and M. E. Baker (2008), Towards an algebra for terrain-based flow analysis, in *Representing, Modeling and Visualizing the Natural Environment: Innovations in GIS*, edited by N. Mount et al., pp. 496, CRC Press, Boca Raton, Fla., USA.

Vidon, P., and A. R. Hill (2004), Denitrification and patterns of electron donors and acceptors in eight riparian zones with contrasting hydrogeology, *Biogeochemistry*, *71*, 259–283.

Vidon, P., and A. P. Smith (2007), Upland controls on the hydrological functioning of riparian zones in glacial till valleys of the Midwest, *J. Amer. Water Resour. Assoc.*, *43*, 1524–1539, doi:10.1111/j.1752-1688.2007.00125.x.

T. J. Grabs, Department of Physical Geography and Quaternary Geology, Stockholm University, SE-106 91, Stockholm, Sweden. (thomas.grabs@natgeo.su.se)

K. G. Jencso and B. L. McGlynn, Department of Land Resources and Environmental Sciences, Montana State University, 334 Leon Johnson Hall, Bozeman, MT, US-59717-3120, USA.

J. Seibert, Department of Geography, University of Zürich, Irchel Winterthurerstr. 190, CH-8057, Zürich, Switzerland.